ORGANIC LETTERS

2003
Vol. 5, No. 5
697−700

Delocalizations in σ-Radical Cations: The Intriguing Structures of Ionized [*n*]Rotanes

Andrey A. Fokin,*,† Peter R. Schreiner,*,‡,§ Sergei I. Kozhushkov,‖ Kurt W. Sattelmeyer,‡ Henry F. Schaefer, III,‡ and Armin de Meijere*,‖

Department of Organic Chemistry, Kiev Polytechnic Institute, pr. Pobedy 37, 03056 Kiev, Ukraine, Department of Chemistry, The University of Georgia, Athens, Georgia 30602-2556, Institut für Organische Chemie, Justus-Liebig University, Heinrich-Buff-Ring 58, D-35392 Giessen, Germany, and Georg-August Universität Göttingen, Institut für Organische Chemie, Tammannstr. 2, D-37077 Göttingen, Germany

aaf@xtf.ntu-kpi.kiev.ua; prs@chem.uga.edu; ameijer1@gwdg.de

Received December 17, 2002

ABSTRACT

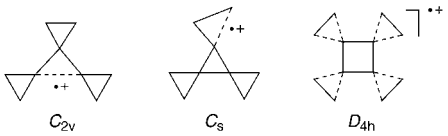

Highly symmetric aliphatic hydrocarbons such as D_{4h}-[4]rotane do not necessarily have degenerate HOMOs. According to our predictions based on high-level computations, its radical cation should display a highly delocalized D_{4h}-symmetric structure, in contrast to its Jahn–Teller distorted cousin, the radical cation of [3]rotane, which exists in two distonic localized forms with C_{2v} and C_s symmetry.

Aliphatic hydrocarbon radical cations are the key intermediates in alkane activations with many chemical and biological oxidizers.[1] Relatively stable alkane radical cations are quite rare, and a better understanding of these species and their reactions is highly desirable. The removal of an electron from a distinct bonding molecular orbital gives so-called σ-radical cations[2,3] with one or several electron-depleted (elongated) σ-bonds. This often leads to quite significant distortions, especially when the electron is taken from a degenerate bonding orbital of a highly symmetrical hydrocarbon, e.g., adamantane,[4] cubane,[5,6] and pagodane.[7] Due to HOMO degeneracies, these systems typically undergo Jahn−Teller (JT) distortions[8] to lower symmetry, followed by a cascade of intricate rearrangements.[6,9−11] Typical examples are cyclopropane and cyclobutane (Scheme 1) for which the HOMOs are doubly degenerate, and the radical cations derived from these are strongly distorted.[12,13] Here we present solid evidence[14,15] for a novel type of highly delocalized alkane σ-radical cation derived from D_{4h}-[4]rotane (**3**), which in

† Kiev Polytechnic Institute.
‡ The University of Georgia.
§ Justus-Liebig University.
‖ Georg-August Universität Göttingen.

(1) Fokin, A. A.; Schreiner, P. R. *Chem. Rev.* **2002**, *102*, 1551.
(2) Roth, H. D.; Weng, H. X.; Zhou, D. H.; Herbertz, T. *Pure Appl. Chem.* **1997**, *69*, 809.
(3) Schmittel, M.; Burghart, A. *Angew. Chem., Int. Ed. Engl.* **1997**, *36*, 2551.
(4) Fokin, A. A.; Gunchenko, P. A.; Peleshanko, S. A.; Schleyer, P. v. R.; Schreiner, P. R. *Eur. J. Org. Chem.* **1999**, *855*, 5.
(5) Qin, X.-Z.; Trifunac, A. D.; Eaton, P. E.; Xiong, Y. *J. Am. Chem. Soc.* **1991**, *113*, 669.
(6) Schreiner, P. R.; Wittkopp, A.; Gunchenko, P. A.; Yaroshinsky, A. I.; Peleshanko, S. A.; Fokin, A. A. *Chem. Eur. J.* **2001**, *7*, 2739.
(7) Prinzbach, H.; Murty, B. A. R. C.; Fessner, W.-D.; Mortensen, J.; Heinze, J.; Gescheidt, G.; Gerson, F. *Angew. Chem., Int. Ed. Engl.* **1987**, *26*, 457.
(8) Bersuker, I. B. *Chem. Rev.* **2001**, *101*, 1067.
(9) Marcinek, A.; Rogowski, J.; Gebicki, J.; Chen, G.-F.; Williams, F. *J. Phys. Chem.* **2000**, *104*, 5265.
(10) Bally, T.; Bernhard, S.; Matzinger, S.; Truttmann, L.; Zhu, Z. D.; Roulin, J.-L.; Marcinek, A.; Gebicki, J.; Williams, F.; Chen, G.-F.; Roth, H. D.; Herbertz, T. *Chem. Eur. J.* **2000**, *6*, 849.
(11) Bally, T.; Truttmann, L.; Dai, S.; Williams, F. *J. Am. Chem. Soc.* **1995**, *117*, 7916.
(12) Du, P.; Hrovat, D. A.; Borden, W. T. *J. Am. Chem. Soc.* **1988**, *110*, 3405.
(13) Wiest, O. *J. Phys. Chem.* **1999**, *103*, 7907.

10.1021/ol027479f CCC: $25.00
Published on Web 02/14/2003

Scheme 1. MP2/6-31G* Frontier Molecular Orbital (FMO) Energies (in eV) for Cyclopropane, Cyclobutane, [3]Rotane (**1**), [3]Radialene (**2**), [4]Rotane (**3**), and [4]Radialene (**4**)

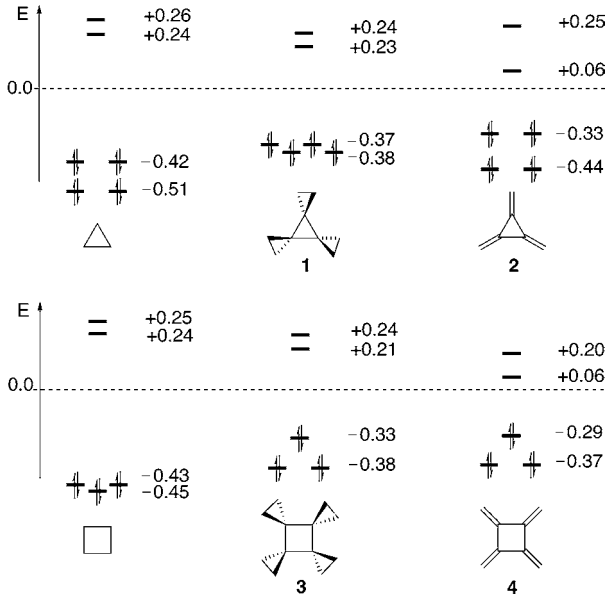

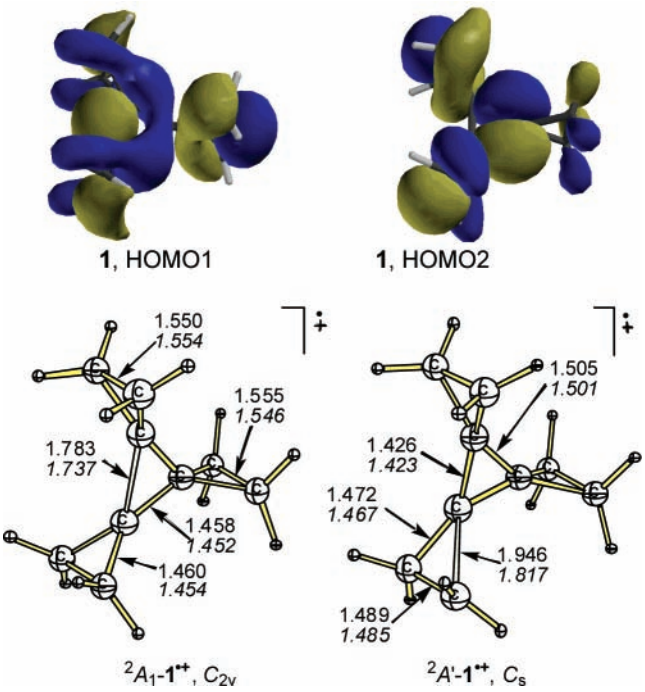

Figure 1. *e*′-HOMOs of **1** and the B3LYP/6-31G* and MP2/6-31G* (italic) geometries of the two forms of the [3]rotane radical cation (**1**$^{\bullet+}$).

contrast to that derived from D_{3h}-[3]rotane (**1**), retains the full symmetry of the parent neutral hydrocarbon. Although ionized species derived from **1** and **3** have been generated[16] and investigated by means of photoelectron spectroscopy (PE), this tells little about the structure of these radical cations (vide infra), in particular, upon adiabatic relaxation.

Our analysis is based on high-level ab initio and density functional theory (DFT) computations that have become an indispensable tool for studying radical cations derived from simple alkanes[17,18] and strained hydrocarbons.[6,13,19−21] For **1**, the computed and the X-ray structural parameters agree very well;[22] the DFT geometry of **3** matches closely the more recent[23] low-temperature X-ray[24,25] crystal structure,[26] as well as lower-level computational[27] data.

The smallest [*n*]rotane, **1**, displays a doubly degenerate HOMO (Scheme 1 and Figure 1); removal of one electron leads to the Jahn−Teller-distorted C_{2v} and C_s forms of the radical cation with either an elongated bond in the inner ring ($^2A_1$-**1**$^{\bullet+}$) or a very long proximal C−C bond in one of the outer rings ($^2A'$-**1**$^{\bullet+}$). The two radical cations have virtually the same energy.

An entirely different situation arises for [4]rotane (**3**): the HOMO of **3** is nondegenerate, and **3**$^{\bullet+}$ (Scheme 1 and Figure 2) can, in principle, maintain the D_{4h}-symmetry of its parent neutral. At the noncorrelated HF/6-31G* level, all delocalized structures of the [4]rotane radical cation [D_{4h}-square (**3**$^{\bullet+}$), D_{2h}-rhombus (**5**$^{\bullet+}$), C_{2v}-trapezium (**6**$^{\bullet+}$), and D_{2h}-parallelogram (**7**$^{\bullet+}$)] are high-order saddle points and only a localized C_s-structure (**8**$^{\bullet+}$) with one very long proximal C−C bond is a minimum (Scheme 2). At correlated levels, however,

(14) All geometries were optimized and characterized at the Becke−3−Lee−Yang−Parr (B3LYP) density functional theory (DFT) and Møller−Plesset (MP2) levels of theory utilizing a 6-31G* basis set; energy single points were computed at B3LYP/6-311+G**//B3LYP/6-31G* and MP2//6-311+G**//MP2/6-31G* and magnetic properties at CSGT-B3LYP/6-311+G**//B3LYP/6-31G*.

(15) Frisch, M. J.; Trucks, G. W.; Schlegel, H. B.; Scuseria, G. E.; Robb, M. A.; Cheeseman, J. R.; Zakrzewski, V. G.; Montgomery, J. A., Jr.; Stratmann, R. E.; Burant, J. C.; Dapprich, S.; Millam, J. M.; Daniels, A. D.; Kudin, K. N.; Strain, M. C.; Farkas, O.; Tomasi, J.; Barone, V.; Cossi, M.; Cammi, R.; Mennucci, B.; Pomelli, C.; Adamo, C.; Clifford, S.; Ochterski, J.; Petersson, G. A.; Ayala, P. Y.; Cui, Q.; Morokuma, K.; Malick, D. K.; Rabuck, A. D.; Raghavachari, K.; Foresman, J. B.; Cioslowski, J.; Ortiz, J. V.; Stefanov, B. B.; Liu, G.; Liashenko, A.; Piskorz, P.; Komaromi, I.; Gomperts, R.; Martin, R. L.; Fox, D. J.; Keith, T.; Al-Laham, M. A.; Peng, C. Y.; Nanayakkara, A.; Gonzalez, C.; Challacombe, M.; Gill, P. M. W.; Johnson, B. G.; Chen, W.; Wong, M. W.; Andres, J. L.; Head-Gordon, M.; Replogle, E. S.; Pople, J. A. *Gaussian 98*, revision A.9; Gaussian, Inc.: Pittsburgh, PA, 1998.

(16) Gleiter, R.; Haider, R.; Conia, J.-M.; Barnier, J.-P.; de Meijere, A.; Weber, W. *J. Chem. Soc., Chem. Commun.* **1979**, 130.

(17) Sulzbach, H. M.; Graham, D.; Stephens, J. C.; Schaefer, H. F. *Acta Chem. Scand.* **1997**, *51*, 547.

(18) Zuilhof, H.; Dinnocenzo, J. P.; Reddy, A. C.; Shaik, S. *J. Phys. Chem.* **1996**, *100*, 15774.

(19) Trifunac, A. D.; Werst, D. W.; Herges, R.; Neumann, H.; Prinzbach, H.; Etzkorn, M. *J. Am. Chem. Soc.* **1996**, *118*, 9444.

(20) Clark, T. *Acta Chem. Scand.* **1997**, *51*, 646.

(21) Sastry, G. N.; Bally, T.; Hrouda, V.; Cársky, P. *J. Am. Chem. Soc.* **1998**, *120*, 9323.

(22) Boese, R.; Miebach, T.; de Meijere, A. *J. Am. Chem. Soc.* **1991**, *113*, 1743.

(23) Almenningen, A.; Bastiansen, O.; Cyvin, B. N.; Cyvin, S.; Fernholt, L.; Rømming, C. *Acta Chem. Scand. A* **1984**, *38*, 31.

(24) Pascard, C.; Prangé, T.; de Meijere, A.; Weber, W.; Barnier, J.-P.; Conia, J.-M. *J. Chem. Soc., Chem. Commun.* **1979**, 425.

(25) Prangé, T.; Pascard, C.; de Meijere, A.; Behrens, U.; Barnier, J.-P.; Conia, J.-M. *Nouveau J. Chim.* **1980**, *4*, 321.

(26) Because of discrepancies between the structural data for [4]rotane in the literature (ref 23 vs refs 24 and 25), we asked Prof. Dr. R. Boese to reinvestigate the X-ray crystal structure; the geometry is in agreement with the one described in ref 23.

(27) Rasmussen, K.; Tosi, C. *J. Mol. Struct.* (*THEOCHEM*) **1985**, *121*, 233.

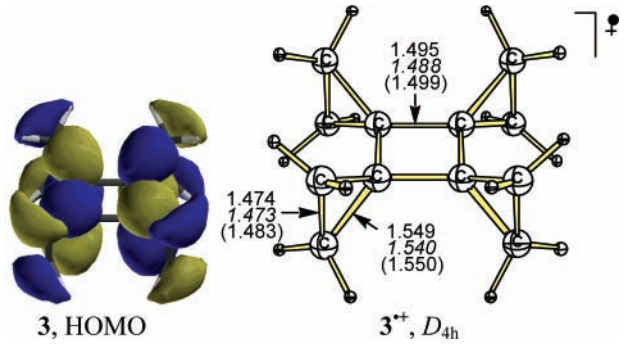

Figure 2. HOMO of **3** as well as the B3LYP/6-31G*, MP2/6-31G* (in italics), and CCSD/cc-pVDZ (in parentheses) computed geometries of **3**•+.

the above structures optimize to a single D_{4h}-symmetric minimum (**3**•+). The B3LYP/6-31G* geometry of D_{4h}-**3**•+ (Nimag = 0) shows substantial shortening of the central cyclobutane (1.495 vs 1.529 Å) and distal cyclopropane (1.474 vs 1.513 Å) C−C bonds; the proximal cyclopropane C−C bonds are elongated in **3**•+ relative to the neutral hydrocarbon **3** (1.549 vs 1.503 Å). Similar results for **3**•+ were obtained with other DFT functionals such as BLYP and BH&HLYP with 6-31G* and larger (6-311+G**) basis sets, as well as at MP2/6-31G*. These structural changes are very different from those of unsubstituted cyclobutane, which gives a C_{2h}-symmetric parallelogram-shaped radical cation upon ionization due to the HOMO degeneracy (Scheme 1).[13] Hence, electron correlation alters this picture

Scheme 2. HF/6-31G* Stationary Points for the [4]Rotane Radical Cation (**3**•+, **5**•+−**8**•+) and Possible Pathways for the Rearrangement of **3**•+ at B3LYP/6-311+G**//B3LYP/6-31G* (Relative Energies in kcal/mol)

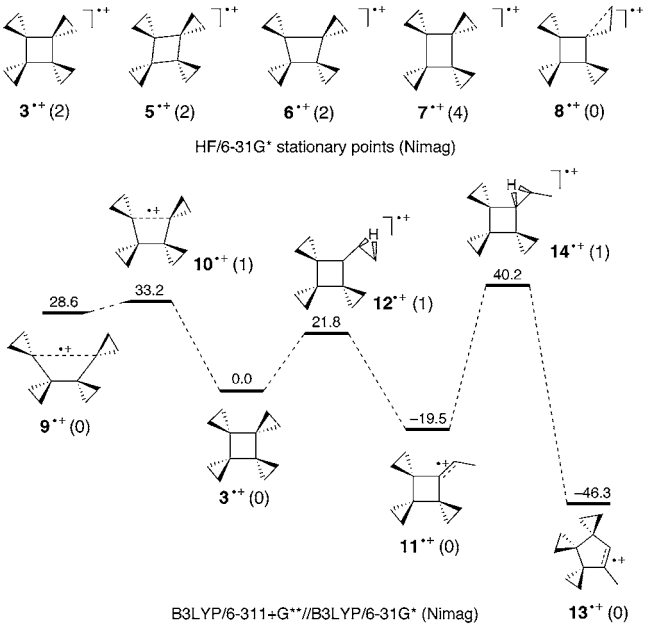

Table 1. Vertical Ionization Potentials for [3]- and [4]Rotane at B3LYP/6-311+G**//B3LYP/6-31G* (Absolute Energies (*E*) in −au)

[*n*]rotane	$E_{neutral}$	$E_{radical\ cation}$	IP_{calc} [kcal/mol]	IP_{calc} [eV]	IP_{exp} [eV][a]
3	350.11402	349.77901	210.2	9.12	9.12
4	466.86716	466.57171	185.4	8.04	8.22

[a] From ref 16.

dramatically: D_{4h}-**3**•+ is a minimum at all correlated levels used here.[28] The orbital ordering shows a substantial energy gap between the nondegenerate HOMO and the next lower-lying, degenerate MOs. As DFT and MP2 may suffer from problems associated with the open-shell nature of **3**•+, it was also optimized at the coupled cluster level of theory to put our initial findings on solid grounds. A recently implemented scheme,[29] which precludes many of the problems that traditionally plague open-shell coupled cluster computations, has been used. Neutral **3** was taken as the reference state, and equation-of-motion (EOM) ionization potential coupled cluster theory was applied to optimize[30] the radical cation at the EOM-CCSD/cc-pVDZ level. Inspection of the updated Hessian matrix identifies D_{4h}-**3**•+ as a minimum. With the confidence usually credited to the coupled cluster approach, one may conclude that **3**•+ indeed is highly symmetrical and that it has the electronic structure depicted above, displaying a nondegenerate HOMO.

Although we noted before that PE spectra are insufficient for drawing conclusions about the structure of a fully relaxed radical cation, a comparison of the computed and measured[16] orbital energies lends confidence to the methods applied here (Table 1); the experimental and computed vertical IPs agree exceptionally well.

There are a number of rearrangement paths for **3**•+; two of them are shown in Scheme 2. Breaking of the central cyclobutane ring endothermically gives **9**•+ via transition structure **10**•+ (barrier = 33.2 kcal/mol). In contrast, the opening of the proximal C−C bond followed by hydrogen shift to the methylenecyclobutane derivative **11**•+ via transition structure **12**•+ is exothermic but involves a substantial barrier (21.8 kcal/mol). Further transformations of **11**•+ to the cyclopentane derivative **13**•+, which is the low-lying minimum for this part of the potential energy surface, are hampered by the very large computed barrier (59.7 kcal/mol associated with transition structure **14**•+). Thus, the D_{4h}-structure of the [4]rotane radical cation **3**•+ is kinetically stable, and it should therefore be observable experimentally.

Eight vicinal C−C bonds participate in the spin/charge delocalization in **3**•+, but the interactions between the

(28) On the basis of the HF results, one may argue that the D_{4h}-[4]rotane radical cation (Nimag = 2) displays vibronic coupling between the ground and exited states. This, however, is not supported by our results on the [4]rotane dication, which, being a closed-shell molecule, is a second-order stationary point at HF, but a minimum at all correlated levels.

(29) Stanton, J. F.; Gauss, J. *J. Chem. Phys.* **1999**, *111*, 8785.

(30) Local version of the ACESII program system was used. Stanton, J. F.; Gauss, J.; Watts, J. D.; Lauderdale, W. J.; Bartlett, R. J. *Int. J. Quant. Chem.* **1992**, *S26*, 879.

p-orbitals of the spiro-carbons are *antibonding* (Figure 2). Hence, the cyclopropyl groups stabilize each electron-deficient spiro-carbon atom individually. The central bonds in $\mathbf{3}^{\bullet+}$ are shorter due to the decrease of the *p*-antibonding character of the b_{2u}-HOMO of **3** after removal of an electron.

The cyclic delocalization of *p*-electrons through the central ring in $\mathbf{3}^{\bullet+}$ is insignificant. The nucleus-independent chemical shifts (NICS, a qualitative measure of aromaticity)[31] computed at the midpoint of $\mathbf{3}^{\bullet+}$ are more positive than those for neutral **3** (8.2 vs 3.2 ppm, respectively), indicating an overall increased σ-antiaromatic character.

The orbital orderings for **1** and **3** are also characteristic for [3]- and [4]radialenes (**2** and **4**, respectively),[32] which are their closest π-analogues (Scheme 1). The NICS of **4** and $\mathbf{4}^{\bullet+}$ are 8.4 and 8.2 ppm (7.8 at PW91/IGLO-III//B3LYP/6-311+G**[33]), respectively, also reflecting the antiaromatic character of these species.[34] In contrast, a NICS value of −20.3 ppm was computed (CSGT-B3LYP/6-311+G**//B3LYP/6-31G*) at the midpoint of the σ-aromatic C_{2v}-pagodane radical cation.[7]

This situation is somewhat reminiscent of simple diatomics where s/p-orbital mixing determines the qualitative MO ordering. Hence, while O_2 and F_2 each have a low-lying σ-bonding π-MO and therefore a degenerate set of π-HOMOs, the situation is reversed in the series from Li_2 to N_2 (Scheme 3). This is due to strong s/p-mixing that promotes the σ-orbital above the p-orbitals. As the rotanes also display large p-coefficients in the spirocyclopropane groups, the σ/π-space mixing determines the orbital order. That this effect only surfaces for **3** derives from the C−C antibonding symmetric nature of the HOMO.

Our comparison of the MO structure of $\mathbf{3}^{\bullet+}$ with that of the cyclobutane radical cation also re-emphasizes that computations at the HF level do not reveal their true nature: at this level, these two radical cations similarly form a number of higher-order stationary points (a selection of these is depicted in Scheme 2). At electron-correlated levels (DFT, MP2, CCSD), these multiple structures converge to a single one for each of the radical cations.

Scheme 3 Qualitative Valence MO Occupations for F_2 and N_2

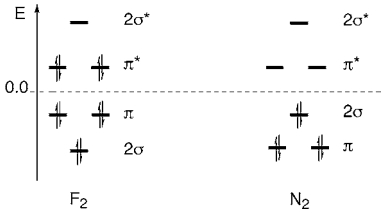

Thus, we identified [4]rotane as a member of a series of highly symmetrical oligocyclic hydrocarbons with non-degenerate HOMOs.[35] The even-numbered members of the [*n*]rotanes and [*n*]radialenes will display the same orbital patterns. As a consequence, the radical cation of these hydrocarbons should also display a *symmetric* structure (at least at low temperatures). We also predict that the removal of the second electron from the respective HOMOs will generate symmetric, saturated hydrocarbon *dications*. These bold predictions anxiously await their experimental verification!

Acknowledgment. This work was supported by the Fonds der Chemischen Industrie, the Deutsche Forschungsgemeinschaft, the Volkswagen-Stiftung, the Petroleum Research Fund, administrated by the American Chemical Society (P. R. S.), the NATO Science Program, the Fundamental Research Foundation of the Ukraine, and the National Science Foundation. We thank Prof. Thomas Bally, Fribourg, Switzerland, for fruitful discussions.

Supporting Information Available: The *xyz*-coordinates for all computed species. This material is available free of charge via the Internet at http://pubs.acs.org.

OL027479F

(31) Schleyer, P. V. R.; Maerker, C.; Dransfeld, A.; Jiao, H.; van Eikema Hommes, N. J. R. *J. Am. Chem. Soc.* **1996**, *118*, 6317.
(32) Griffin, G. W.; Peterson, L. I. *J. Am. Chem. Soc.* **1963**, *85*, 2268.
(33) Schleyer, P. V. R.; Manoharan, M.; Wang, Z.-X.; Kiran, B.; Jiao, H.; Puchta, R.; van Eikema Hommes, N. J. R. *Org. Lett.* **2001**, *3*, 2465.
(34) Bally, T.; Buser, U.; Haselbach, E. *Helv. Chim. Acta* **1978**, *61*, 38.
(35) Similar orbital patterns are typical for D_{nh}-symmetrical propellanes for which the HOMO describes the central C−C bond and for some other strained hydrocarbons (diademane, hexaprismane, trishomobarrelene).